Supplementary Materials for

Scalable Functionalized Liquid Crystal Elastomer Fiber Soft Actuators with Multi-Stimulus Responses and Photoelectric Conversion

Dingsheng Wu,[a,b,l] Yanan Zhang,[a,l] Hanrui Yang,[a] Anfang Wei,[b] Yuxin Zhang,[a] Mensah Alfred,[a] Rui Yin,[a] Pengfei Lv,[a, c, d,*] Quan Feng,[b,*] and Qufu Wei[a,*]

Affiliations

[a] Key Laboratory of Eco-Textiles, Ministry of Education, Jiangnan University, Wuxi 214122, P. R. China.

[b] Key Laboratory of Textile Fabrics, College of Textiles and Clothing, Anhui Polytechnic University, Wuhu 241000, P. R. China.

[c] Key Laboratory of Advanced Energy Materials Chemistry (Ministry of Education), Nankai University, Tianjin 300071, P. R. China.

[d] State Key Laboratory of Biobased Material and Green Papermaking，Qilu University of Technology，Shandong Academy of Sciences, Jinan 250353, P. R. China.

* Corresponding authors:
E-mail address: qfwei@jiangnan.edu.cn (Q. W.); pengfeilv@jiangnan.edu.cn (P. L.); fengquan@ahpu.edu.cn (Q. F.)

Keywords: liquid crystal elastomer, MXene, fiber actuators, multiresponsive, adaptive smart window

Table of Contents

1. Experimental Procedures

1.1 Materials

1.2 Synthesis

1.3 Measurements and Characterization

1.4 Actuation Performances of Fiber Actuator

2. Supplementary Figures and Table

3. Captions of Supplementary Videos

1. Experimental Procedures

1.1. Materials

1,4-bis-[4-(3-acryloyloxypropyloxy)benzoyloxy]-2-methylbenzene (RM257) was received from Shijiazhuang Yesheng Chemical Technology Co. Ltd. (Hebei, China). Aluminum titanium carbide, lithium fluoride (LiF), hydrochloric acid (HCl, 36 wt% in H_2O), dichloromethane (CH_2Cl_2), sodium hydroxide (NaOH), 1,6-hexanedithiol (HDT), 2-hydroxy-4'-(2-hydroxyethoxy)-2-methylpropiophenone (HHMP), ethanol, pentaerythritol tetra (3-mercaptopropionate) (PETMP), titanium aluminium carbidewere MAX powder (Ti_3AlC_2, 400 mesh) obtained from Aladdin Reagent Co., Ltd. (Shanghai, China). Dipropylamine (DPA), dopamine hydrochloride and chloroform ($CHCl_3$) were purchased from Sinopharm Chemical Reagent Co., Ltd. (Shanghai, China).

1.2. Synthesis

Synthesis of single-layer $Ti_3C_2T_x$ MXene: Ti_3AlC_2 MAX powder (400 mesh) was dispersed in deionized water three times by magnetic stirring to fully remove small particles. A hydrofluoric acid solution with a concentration of 9 mol/L was prepared through adding an appropriate amount of lithium fluoride to hydrochloric acid and stirring at 4000 rpm for 30 min. 1 g of size-selected Ti_3AlC_2 powder was slowly added to the above etching solution. After etching at 35 °C for 36 h, the solution was washed with deionized water and repeatedly centrifuged at 3500 rpm for 5 min until the supernatant reached pH of ~6. The self-delaminated single-layer MXene flakes were then collected by centrifugation several times at 3500 rpm for 5 min. The dark green supernatant was further centrifuged at 10000 rpm for 10 min to attain sediment containing MXene flakes.

Fabrication of polydopamine-modified MXene (PDA@MXene) ink: First of all, a 2 g/L

concentration of dopamine hydrochloride solution was added dropwise to the $Ti_3C_2T_x$ aqueous dispersion of the same concentration at the predetermined mass ratios ($Ti_3C_2T_x$: dopamine hydrochloride was 10:1). After that, the dispersion was further stirred (300 rpm, 35°C) for 1.5 h and centrifuged (3500 rpm, 5 min) to remove the unreacted monomers in the solution. The sediment was re-dispersed in deionized water by ultrasound to obtain the polydopamine-modified MXene ink (PDA@MXene).

Fabrication of PDA@MXene/LCE fiber actuator: In this experiment, LCE fibers were manufactured through using dry spinning and chemical modification method. First of all, the liquid crystal monomer (RM257, 19.425 g), chain extender (HDT, 2.705 g) and crosslinker (PETMP, 2.931 g) were dissolved in CH_2Cl_2 solvent, and a homogeneous mixed solution with a mass fraction of 24% was prepared by magnetic stirring for 2 h at room temperature. Meantime, the molar ratio of acrylate groups in RM257 and thiol groups in HDT and PETMP was 1.1:1. Subsequently, DPA (1.214 g) was added as a catalyst to the above solution for 15 min to cause the system to undergo a Michael addition reaction. Afterwards, the dry spinning solution is generated by dissolving the photoinitiator (HHMP, 2.023 g) in the 1st step cross-linking solution system.

And then the spinning solution is placed in a syringe and extruded from a nozzle with a diameter of 0.3 mm onto the surface of the PTFE receiving roller. At the same time, the extrusion speed of the syringe and the rotating speed of the receiving roller were set to 1.5 mL/min and 4.8 m/min, respectively. The spinning fibers were treated at a temperature of 80 °C for 15 min, the solvent was evaporated and the fibers were cured. In the 2nd step cross-linking, the LCE fibers are then stretched to different times (1.5, 2.0, 2.5 and 3.0) of their initial length through regulating different rotation speeds of the two rollers, and the stretched fibers

are collected on the surface a second PTFE rotating cylinder. During the stretching the macromolecular chains or liquid crystal units of the fibers aligned and possessed high degrees of orientation along the fiber axes, and the fiber morphology gradually presented a transparent state. Meanwhile, the stretched LCE fibers are irradiated with an ultraviolet lamp (15 mW/cm^2) with a wavelength of 365 nm for 30 min to make the liquid crystal elastomer fiber undergo the 2nd step cross-linking reaction, so as to fix the arrangement direction of liquid crystal units and molecular chains of the LCE fiber. Subsequently, we measured and analyzed the actuation strain and actuation velocity of as-prepared LCE fibers under different drawing ratios, and determined the optimal fiber drawing ratio. The designed LCE fibers were treated by plasma technique with RF level at HI for 1 min, followed by immersion mono-layers of PDA@MXene ink. Finally, the saclable LCE/MXene fibers were prepared under drying condition.

1.3. Measurements and Characterization

A scanning electron microscope (SEM, S4800) and elemental energy spectrometer (EDX) were applied to determine micro-morphological structure and element distribution of different liquid crystal elastomer (LCE) fibers. Transmission electron microscopy (TEM), laser raman spectroscopy (LRS), UV-visible spectrophotometer and X-ray photoelectron spectroscopy (XPS, PHI Quantera II) were implemented to characterize the morphological and chemical structural changes during the modification of MXene. Fourier transform infrared spectroscopy (FTIR) and differential scanning calorimetry (DSC) were used to measure the chemical structure and phase transition temperature of various LCE fibers. Thermogravimetric analysis (TGA) was carried out to investigate the thermal stability of different samples. Polarizing microscope (POM) were used to identify the molecular crystallinity and orientation of various liquid crystal elastomer fibers. A uniaxial testing machine (PT-1198 GDT) was used to confirm

the stress-strain characteristics of different samples.

1.4. Actuation performances of fiber actuator

Thermal actuate properties: To measure the thermal actuation properties of different liquid crystal elastomer fibers, the LCE fibers were first placed in a constant temperature oven at different temperatures. It was held at each temperature for 5 min until the temperature inside the chamber was stable. Then, we took images with a digital camera (Canon 80D) and characterised the length and actuating deformation rate of the LCE microfiber under different temperature by using the Kinovea software to analyze the images. The actuation strain is calculated as illustrated in **Formula S1**[1].

$$S = \frac{L_0 - L_1}{L_0} \times 100\% \quad (1)$$

Where S present actuation strain, L_0, L_1 represents the initial length before heating and the final length after heating of LCE microfibre, respectively.

Light/electric actuate properties: To investigate NIR photothermal actuating properties of LCE fibers, the photothermal actuation strain and temperature changes of different LCE fibers were recorded by a digital camera (Canon 80D) and an infra imaging system (IRC, R500Ex-Pro-D, Japan) under 808 nm NIR light irradiation. In addition, the PDA@MXene/LCE fiber with a length of 10 cm was connected to the positive and negative electrodes of the small experimental power supply, and the current change on the LCE fiber is controlled by changing the values of voltage. At the same time, a digital camera and infrared imaging system were used to record the electro-thermal actuation strain and temperature change of the fiber actuator, and then the electrothermal driving performances of the fiber were analyzed.

2. Supplementary Figures and Table

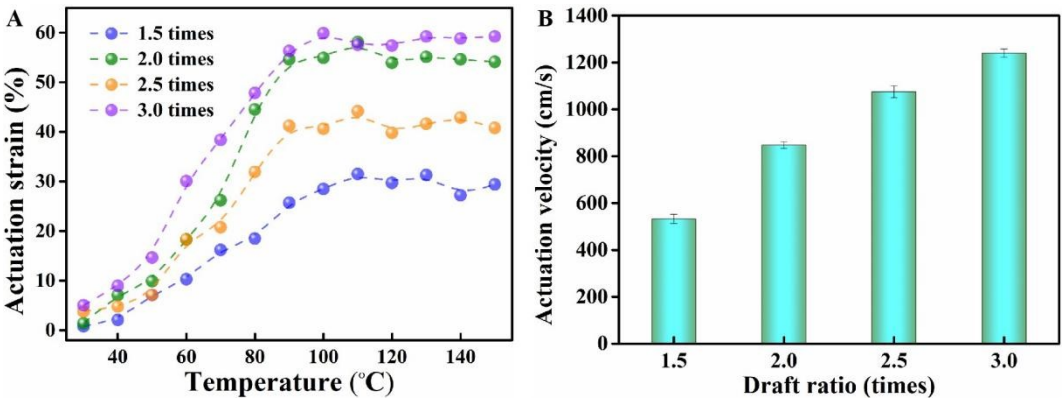

Fig. S1 Actuation strain (A) and actuation velocity (B) of the as-prepared LCE fiber actuator with different drawing ratios.

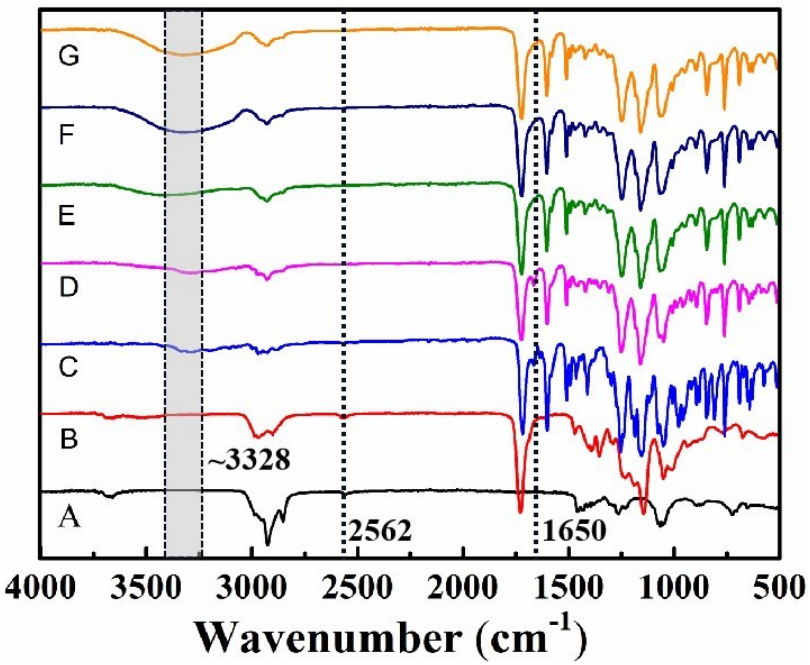

Fig. S2 FT-IR analysis of (A) HDT, (B) PETMP, (C) RM257, LCE fiber before (D) and after (E) UV crosslinking modification, (F) LCE fiber modified by plasma technique, (G) the PDA@MXene/LCE fiber soft actuator.

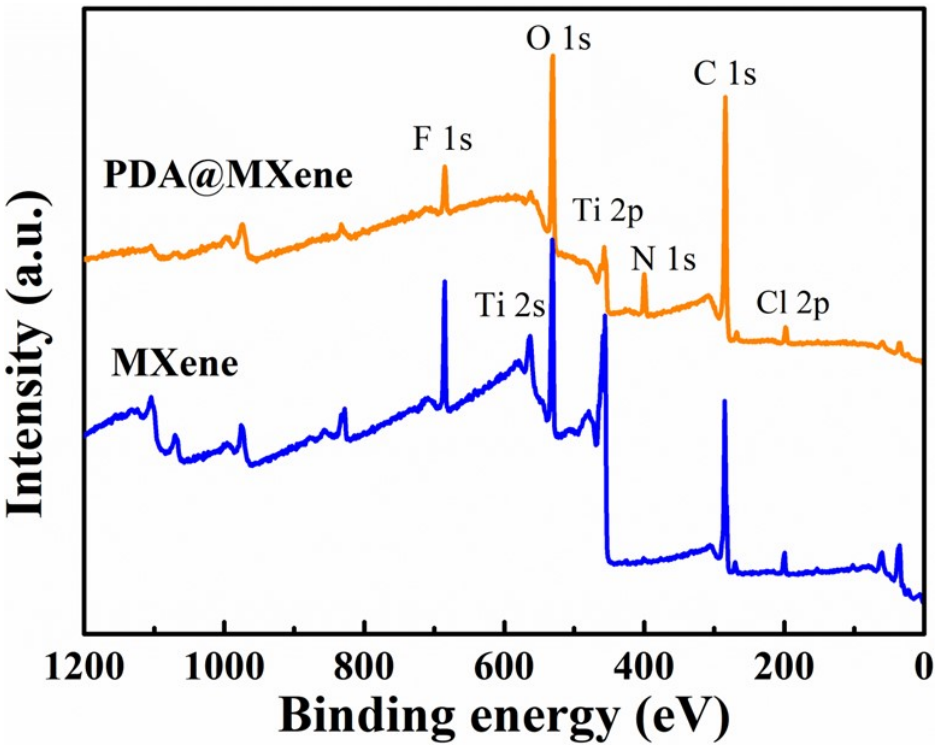

Fig. S3 XPS spectra of the MXene and PDA@MXene nanosheets.

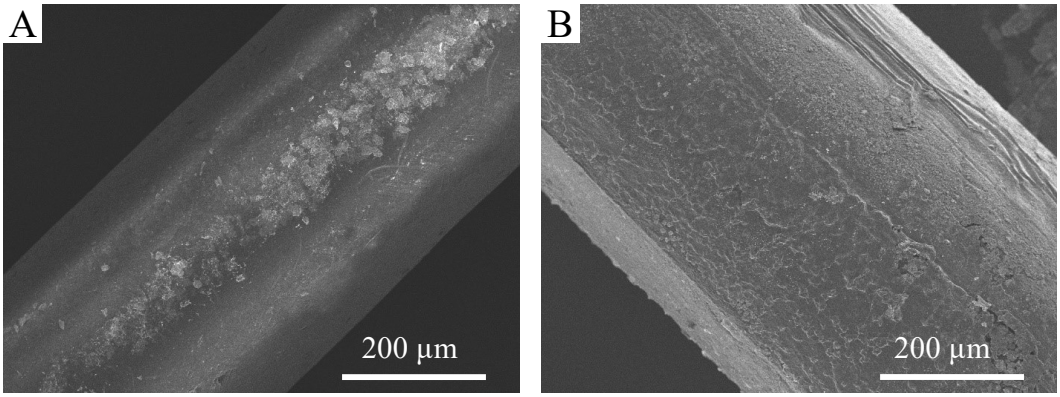

Fig. S4 The surface morphological structure of the LCE fiber (C) and PDA@MXene/LCE fiber actuator (D).

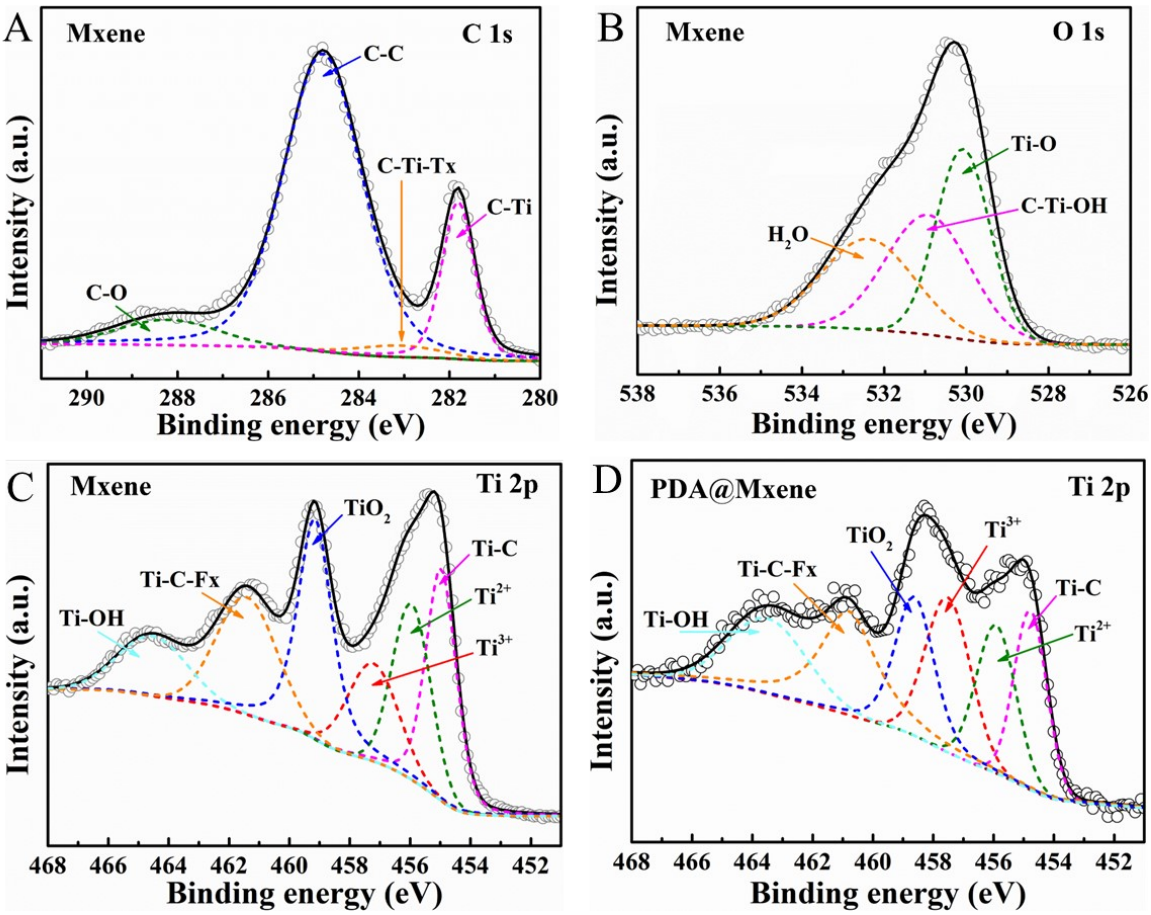

Fig. S5 X-ray photoelectron spectroscopy spectra of (A) C 1s, (B) O 1s, (C) Ti 2p of MXene sheets, (D) Ti 2p of PDA@MXene sheets.

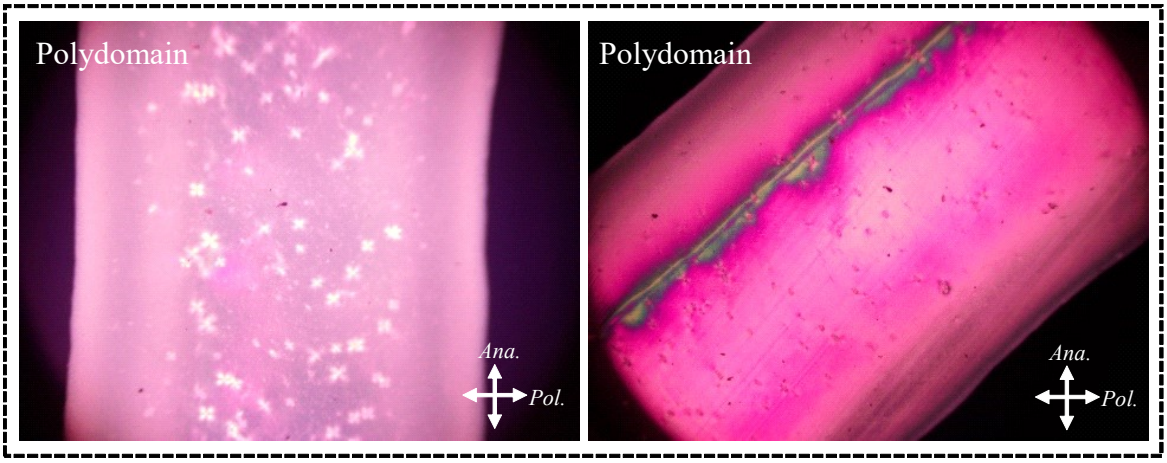

Fig. S6 POM results of prepared polydomain LCE fibers viewed at two different angles with respect to the analyzer.

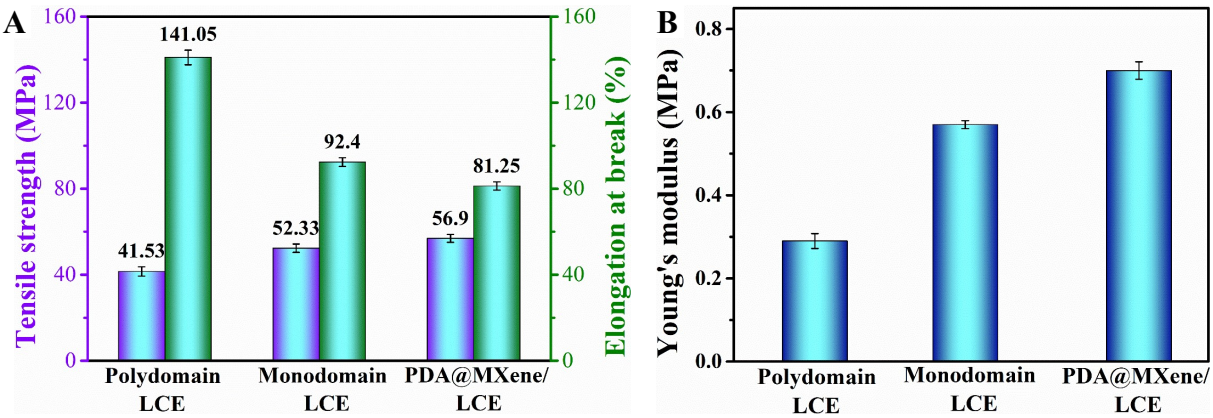

Fig. S7 Tensile breaking strength, elongation at break (A) and Young's modulus (B) diagram of the polydomain LCE fiber, the monodomain LCE fiber, the PDA@MXene /LCE fiber.

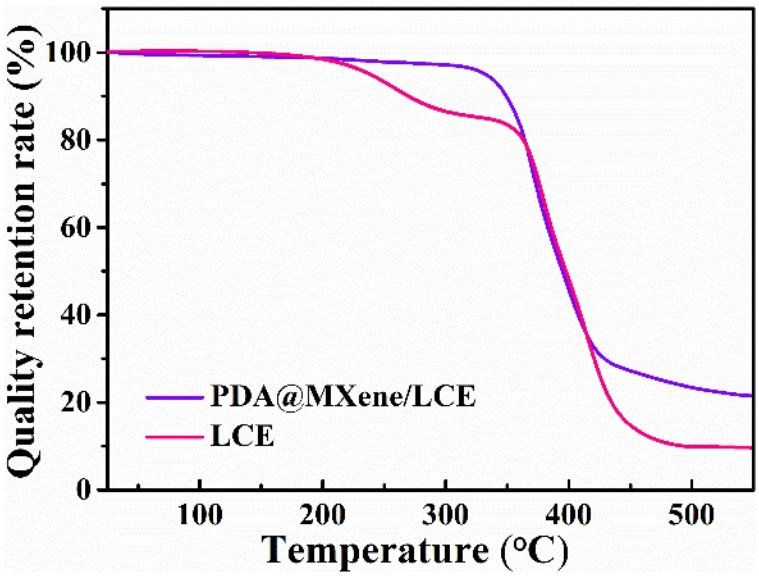

Fig. S8 Thermogravimetric curves of LCE and PDA@Mxene/LCE fibers actuator.

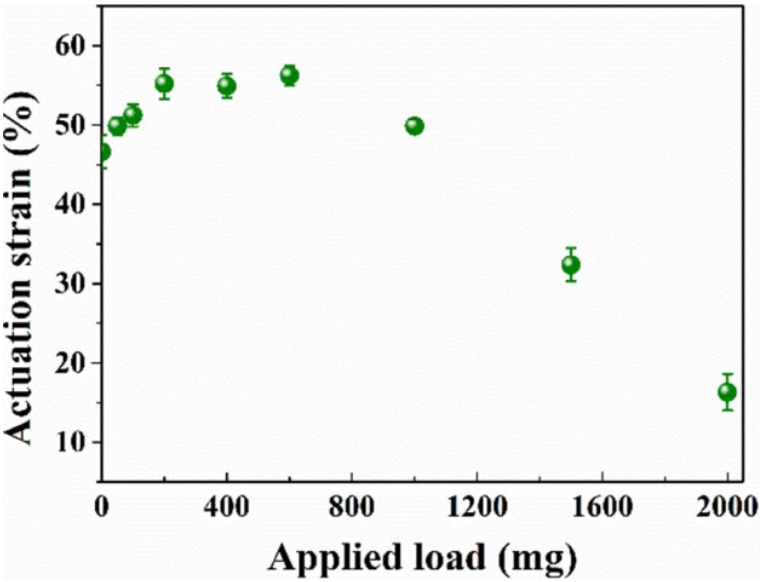

Fig. S9 The relationship between the actuation strain of LCE fiber actuator and different applied loads.

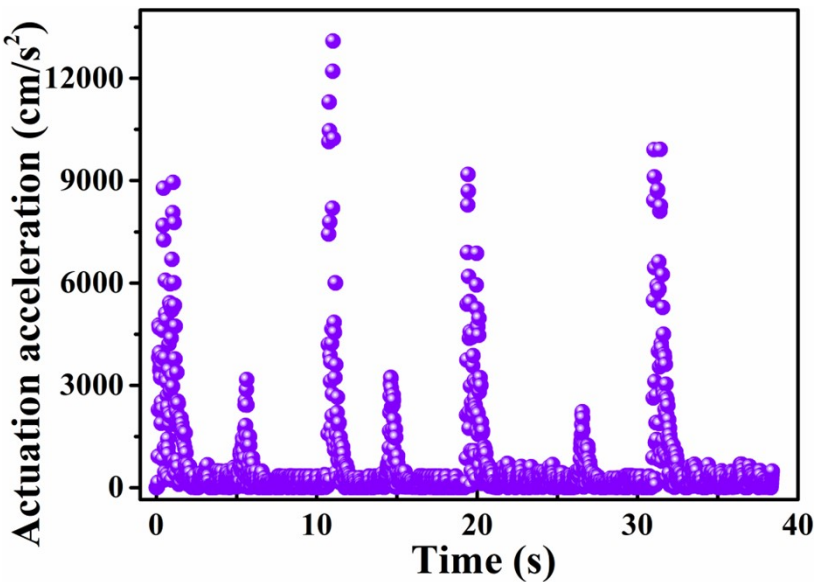

Fig. S10 Image of relationship between thermal actuation acceleration of LCE fiber actuator and time.

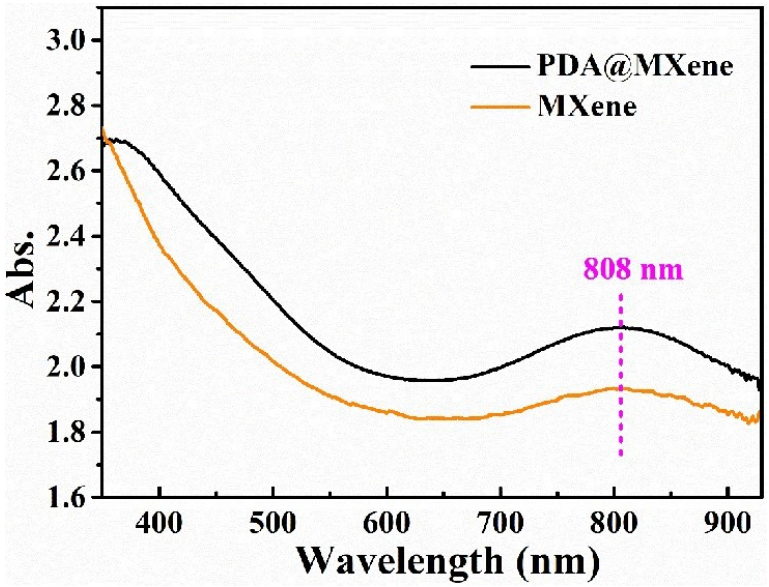

Fig. S11 UV-Vis absorption spectra of the MXene and PDA@Mxene nanomonomer dispersions in deionized water.

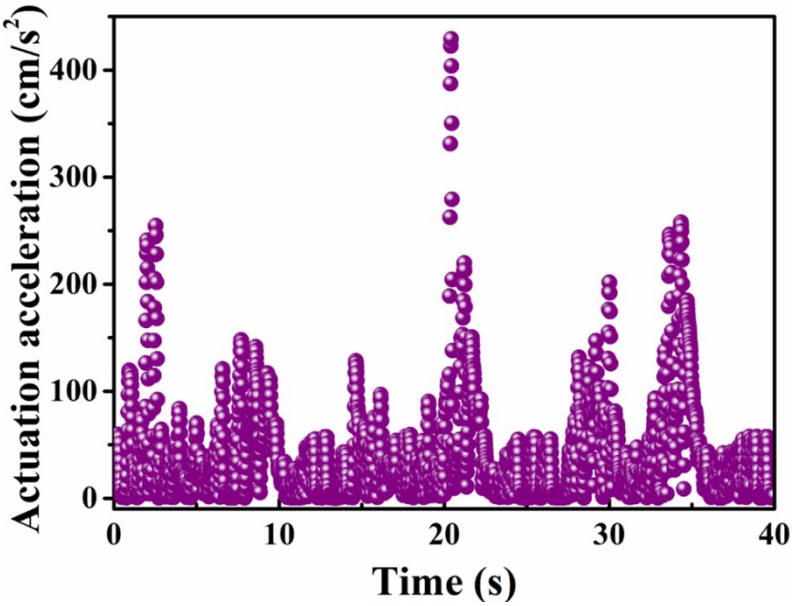

Fig. S12 Image of relationship between NIR light actuation acceleration of PDA@MXene/LCE fiber actuator and time.

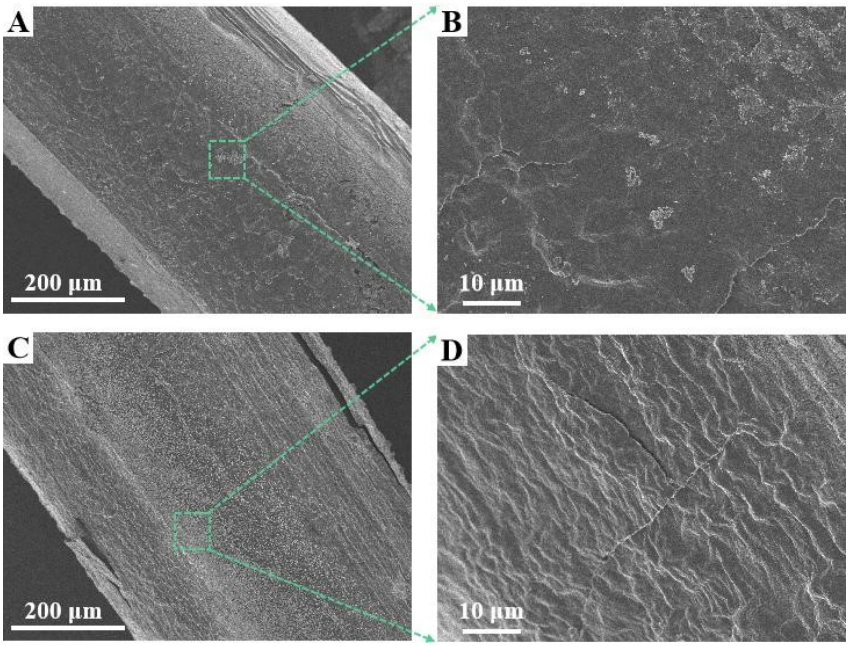

Fig. S13 The surface morphological structure of the PDA@MXene/LCE fiber actuator before (A, B) and after (C, D) 100 times of near-infrared light actuation deformation.

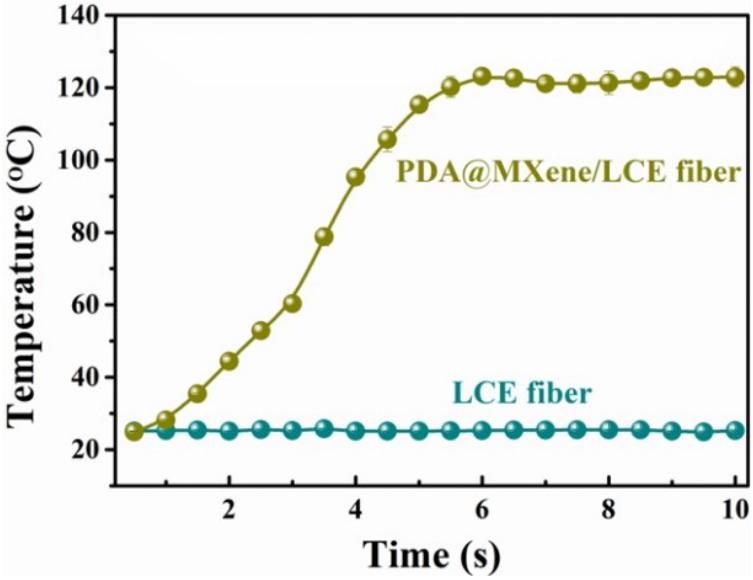

Fig. S14 Electrothermal temperature of LCE fiber actuator and PDA@MXene/LCE fiber actuator under continuous electrical stimulation of 4 V for 10 s.

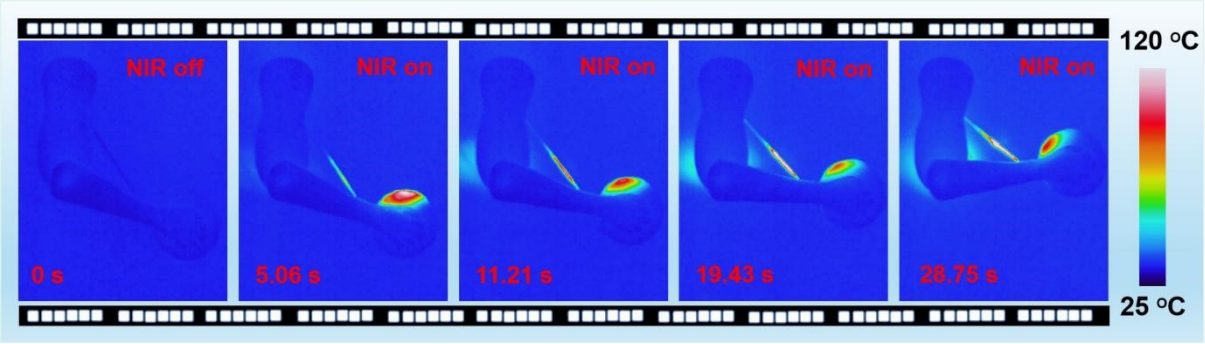

Fig. S15 Infrared image of driving process of NIR light controlled artificial muscle model constructed by using the PDA@MXene/LCE fiber actuator under continuous light stimulation of 7000 W/m^2.

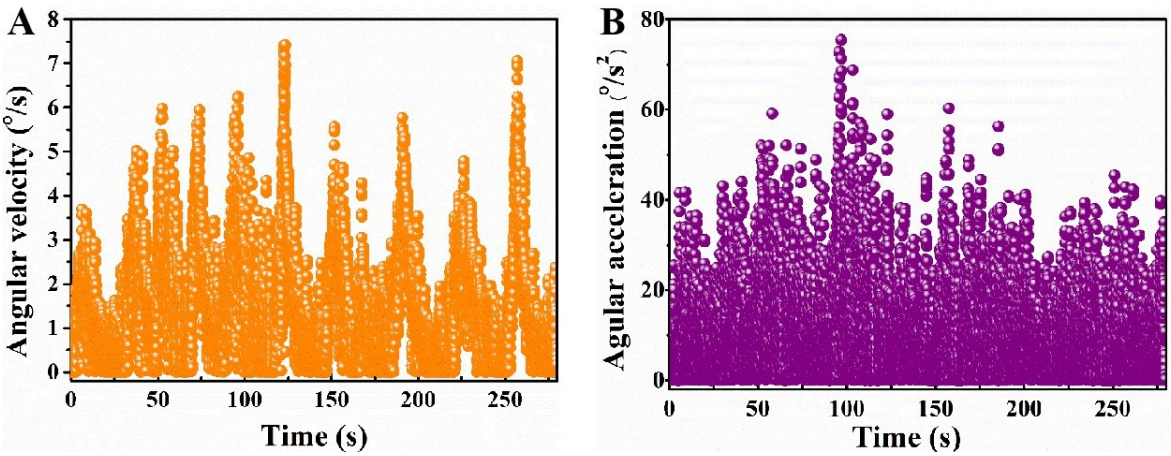

Fig. S16 Image of angular velocity (A) and angular acceleration (B) of NIR light controlled artificial muscle model under continuous light stimulation.

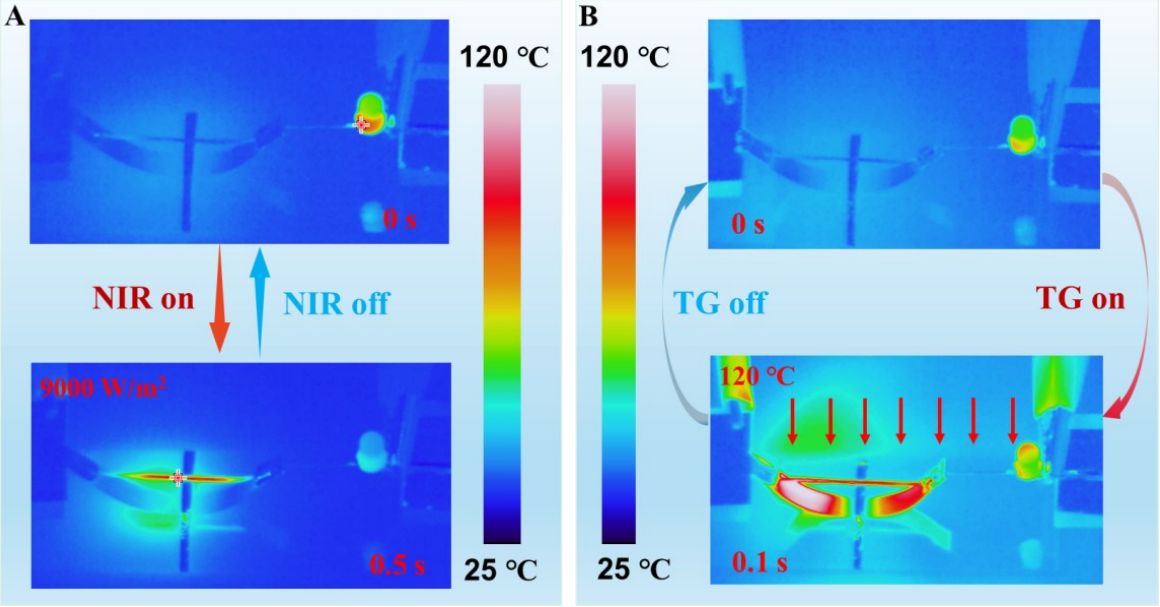

Fig. S17 Infrared image of near-infrared light (A) /temperature (B) control intelligent circuit switch

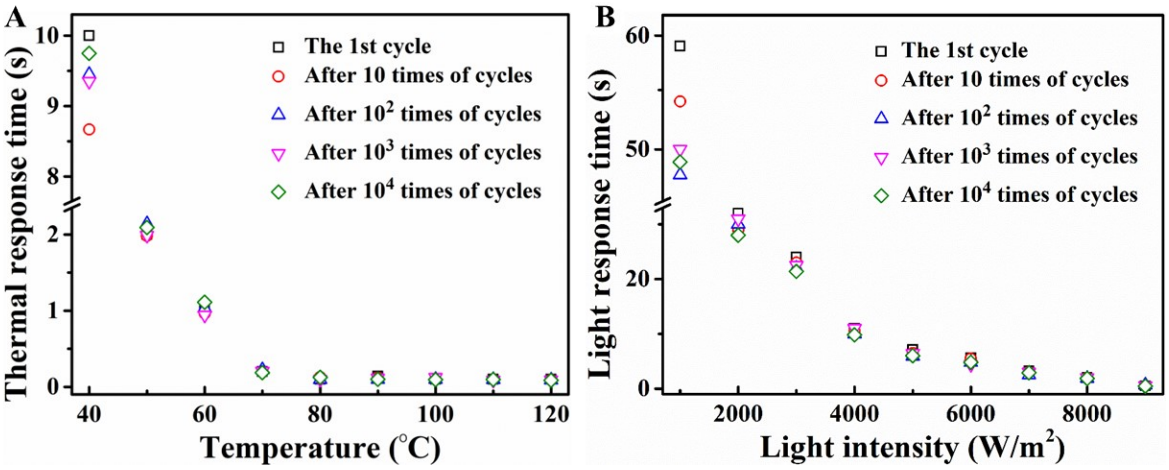

Fig. S18 Response time of photo and thermal smart circuit switch after 10, 10^2, 10^3 and 10^4 cycles at different temperatures (A) and light intensity (B).

Table S1. Actuation performances and applications of the PDA@MXene/LCE fiber actuator in comparison with reported literature.

Materials	Method & Strategy	Thermal-actuate response (actuate rate/ time)	Light-actuate response (actuate rate/ time)	Electro-actuate response (actuate rate/ time)	Application
LM-LCE composite fibers[2]	dry spinning	N/R	N/R	40%/ 10 s	electronically control artificial muscle
LM-LCE fiber[3]	4D printable	11-20%/ 180 s	5%/ 25 s	5-12%/ 15-30 s	NIR light control switch
LCE fibers[4]	direct ink write printing	51%/ N	N/R	N/R	thermal control artificial muscle
LM-LCE coaxial fiber[5]	3D direct ink printing	N/R	N/R	50%/ 20 s	self-sensing 3D soft robot
PDA-coated LCE microfiber[6]	electro -spinning technique	33-55%/ 0.2 s	10-20%/ 0.4 s	N/R	microtweezer, microswimmer, microsoft pump

LLCP fibers[7]	shaping drafting technique	N/R	81%/ 16 s	N/R	light-driven hinges; spider webs
CNTs/LCE core-shell fibers[8]	shaping drafting technique	45%/ 8 s	20-30%/ 20-50 s	N/R	photo-induced artificial muscle，optical gripper
Twisted GO/LCE fibers[9]	shaping drafting technique	N/R	50-70 %/ 0.4 s	N/R	photo controlled self-oscillator
Twisted LCE fiber[10]	shaping drafting technique	40%/ 4 s	N/R	N/R	rotating microengines
PDA@MXene/LCE fibers (this work)	**dry spinning drafting technique**	**50-60%/ 0.4 s**	**40-50%/ 5 s**	**40-50%/ 4 s**	**light controll artificial muscle, smart circuit switch, adaptive smart window system**

3. Captions of Supplementary Videos

Supplementary Video S1: Thermal Actuation Process of the LCE Long Fiber Actuator.

Supplementary Video S2: The PDA@Mxene/LCE Composite Fiber Actuator Driven by 808 nm NIR Light.

Supplementary Video S3: NIR Light Controlled Artificial Muscle Constructed with the PDA@ Mxene/LCE Composite Fiber.

Supplementary Video S4: The PDA@Mxene/LCE Composite Fiber Based NIR Light and Thermal Controlled Smart Circuit Switch.

Supplementary Video S5: Adaptive Smart Window System Integrated by Light-Driven Curtain with Solar Cells.

References

1. J. Zhang, Y. Guo, W. Hu, R. H. Soon, Z. S. Davidson and M. Sitti, *Adv. Mater.*, 2021, **33**, e2006191.
2. J. Sun, Y. Wang, W. Liao and Z. Yang, *Small*, 2021, **17**, e2103700.
3. C. P. Ambulo, M. J. Ford, K. Searles, C. Majidi and T. H. Ware, *ACS Appl. Mater. Interfaces*, 2021, **13**, 12805-12813.
4. D. J. Roach, C. Yuan, X. Kuang, V. C. Li, P. Blake, M. L. Romero, I. Hammel, K. Yu and H. J. Qi, *ACS Appl. Mater. Interfaces*, 2019, **11**, 19514-19521.
5. A. Kotikian, J. M. Morales, A. Lu, J. Mueller, Z. S. Davidson, J. W. Boley and J. A. Lewis, *Adv. Mater.*, 2021, **33**, e2101814.
6. Q. He, Z. Wang, Y. Wang, Z. Wang, C. Li, R. Annapooranan, J. Zeng, R. Chen, S. Cai, *Sci. Robot.* 2021, **6**, eabi9704.
7. X. Pang, L. Qin, B. Xu, Q. Liu and Y. Yu, Adv. Funct. Mater., 2020, **30**.
8. Y. Yu, L. Li, E. Liu, X. Han, J. Wang, Y.-X. Xie and C. Lu, *Carbon*, 2022, **187**, 97-107.
9. Z. Hu, Y. Li and J. A. Lv, *Nat. Commun.*, 2021, **12**, 3211.
10. Y. Wang, J. Sun, W. Liao and Z. Yang, *Adv. Mater.*, 2022, **34**, e2107840.